



Investigating the effect of drawing process parameters on borosilicate glass fiber thickness

Cennet Yıldırım^{1,2,#,*}, Eda Turgut^{1,3,#}, Sedat Sürdem⁴, Abdülkerim Yörükoğlu¹

¹Turkish Energy, Nuclear and Mineral Research Agency, Boron Research Institute, Ankara, 06530, Turkey

²Istanbul Technical University, Graduate School of Natural and Applied Sciences, Department of Metallurgical and Materials Engineering, Istanbul, 34469, Turkey

³Gazi University, Graduate School of Natural and Applied Sciences, Department of Chemical Engineering, Ankara, 06530, Turkey

⁴Gazi University, Graduate School of Natural and Applied Sciences, Department of Environmental Sciences, Ankara, 06570, Turkey

ARTICLE INFO

Article history:

Received June 16, 2021

Accepted January 2, 2022

Available online March 29, 2022

Research Article

DOI: 10.30728/boron.953341

Keywords:

Borosilicate glass

Fiber drawing

Glass fiber

ABSTRACT

Borosilicate glasses have many usage areas due to their high thermal and chemical resistance with a very low thermal expansion coefficient. The number of waste borosilicate glasses is increasing in direct proportion to their usage areas. Creating new usage areas by recycling these glasses will provide cost savings. In this paper, the fiber drawing method is used to recycle borosilicate glass. The aim of this article is to investigate the effect of winding speed and temperature of drawing process on fiber thickness. The fiber drawing process was performed at specific temperatures (1100, 1200, and 1300°C) and at specific winding speeds (50, 175, and 300 rpm). In this context, the thermal behavior of borosilicate glasses was determined by DSC and TGA analysis. The structural and chemical properties and corrosion resistance of borosilicate glass fibers were examined by SEM, XPS, and corrosion test, respectively. The results show that the fiber thickness increased with the increase in the amount of material fed in the crucible, while it decreased with the increase of fiber drawing speed and time.

1. Introduction

The drawing of glass, even older than glass blowing, is an ancient technology. However, glass fiber mass production started in 1893 when Edward Drummond Libbey made clothes from fabric combining silk and fiberglass [1]. After the starting of the mass production process, the use of glass fiber has become increasingly widespread. Glass fibers can be used in many applications, which can be divided into four basic categories: (a) filtration media, (b) insulations, (c) optical fibers, and (d) reinforcement for composite materials [2].

Fiber drawing was first used in air filtration systems. The diameter of fibers used in these systems is significant. Thick fibers provide high porosity and reduce the pressure drop, while thin fibers increase the filtration efficiency [3]. More filtration is provided with the reduction of fiber diameters. Over time, organic polymer fibers have started to replace glass fibers in filtration systems. The use of glass fibers in thermal insulation, which is the second important market share, has started to increase rapidly. Insulation is not only related to the thermal conductivity of the fiber but also to its density. Fiber density is directly proportional to the entrapped air. The rate of entrapped air is related to the fiber diameter and configuration, depending on

the fiber drawing [4]. The diameters of the fibers used in insulation vary between about 5-30 µm. In optical fibers, which is the third important area of use, a larger fiber diameter (>100 µm) is used than insulation fiber. The use of glass fibers in the field of optics has initiated a revolution in information technologies [5].

The fourth most important application area of glass fibers is composite materials, where they are used as reinforcements for polymers. The number of defects reduces with the increase of the surface to volume ratio of glass materials, and thus the strength of glass increases. Therefore, thin diameter filaments are very significant to manufacture high strength composite materials [6].

With the expansion of usage areas, many studies have been made about fiberglass. In recent times, the focus of research has been on developing glass fibers for material reinforcement in composite materials and the wide variety of usage areas [7,8]. Although glass fibers have lower mechanical properties than that of carbon fibers, they are widely used since their raw materials are inexpensive and they have a facile production process [9-11].

Brøndsted et al. [12] have focused on why glass fiber composites take first place as the most widely used

Authors contributed equally

*Corresponding author: Cennet.Yildirim@tenmak.gov.tr

material. They investigated the properties of glass fibers such as high strength, relatively low density, high hardness, high thermal resistance, high chemical resistance, and low cost [13-17].

Glass fiber production is carried out by drawing, expansion, and curing processes, respectively. Firstly, the glass pieces are heated up to the softening point in the induction furnace before the fiber drawing process. It is then pulled and wound in the form of fibers on a rapidly rotating spinning drum [18].

In literature, studies were done on what can be effective during the drawing of a single fiber [19-22]. As a result of these studies, parameters were investigated, such as non-axial symmetrical effects during fiber drawing, radiation heat transfer between fibers, the effect of airflow, inhomogeneity of conditions between fibers [23,24].

Liu and Banta [25] have developed an analytical model on the parameters that are effective during fiber drawing. Furthermore, Lima and Monteiro [26] and Gupta et al. [27] investigated the thermal behaviors of borosilicate glass/fiber depending on the temperature. As a result of these studies, it was seen that changes in processing temperature affect not only the fiber diameters but also the chemical composition that changes depending on the evaporation of boron oxide. Fiber diameter can also be controlled by the fiber winding speed.

In the present study, the effect of winding speed and temperature of the drawing process on fiber thickness was investigated by keeping the feed amount constant in transforming borosilicate glass into fiber form.

2. Materials and Methods

2.1. Sample Preparation

Waste borosilicate glasses were re-melted and transformed into the fiber. The IF_1450_50 model glass fiber production system, whose design belonged entirely to TENMAK-Boron Research Institute and was produced by MSE Technology (Turkey), was used to draw borosilicate fibers (Figure 1).

The device has an induction melting system. The maximum operating temperature is 1450°C and a platinum-rhodium (Pt-Rh) alloy crucible is used as sample

conat. There are 5 nozzles on the crucible and each nozzle is approximately 0.5 mm in diameter. Fiber drawing system of the device has planar motion in x and y directions, rotational motion and protection covers.

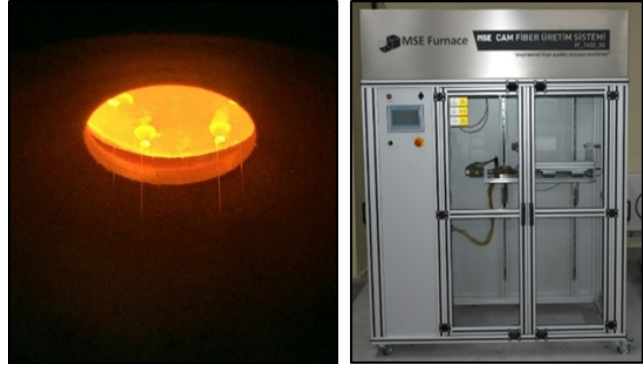


Figure 1. Glass fiber production system.

The borosilicate glasses required for this study were obtained from recycled glasses in our laboratories. The borosilicate glasses were broken into small pieces. As shown in Figure 2, approximately 115 grams of glass pieces were added into the platinum-rhodium (Pt-Rh) alloy crucible.

As the fiber drawing time increases, the amount of material remaining in the crucible decreases. The fiber thickness decreases significantly, and ruptures occur with the decrease in the amount of material. Hence 115 grams of glass pieces, the maximum amount of material used in the crucible, were used for each operating temperature. Borosilicate glass fibers were drawn at the temperatures and winding speeds given in Table 1.

Table 1. The operating temperatures and winding speeds.

Temperature (°C)	Winding Speed (rpm)		
1100	50	175	300
1200	50	175	300
1300	50	175	300

The molten glass inside the crucible is drawn through many nozzles downwards into the air, forming more viscous fiber. Then, the fiber is cooled as it proceeds



Figure 2. The production steps of the borosilicate glass fiber: breaking into small pieces, remelting, and drawing, respectively.

through the air, and the fiber is wound around the drum. Samples were taken at different periods, at 10 minutes, 30 minutes, and 1 hour after fiber drawing started. After about 2 hours of fiber drawing, the amount of material remaining in the crucible was weighed. Finally, the characterization analysis of the drawn fibers was performed.

2.2. Characterization Techniques

Thermal analysis was performed to evaluate the thermal behavior of obtained borosilicate glasses using platinum crucible in an argon (Ar) atmosphere, and at a heating rate of 10 K/min from 25°C to 1300°C via Netzsch STA 449 F3 Jupiter.

X-ray photoelectron spectroscopy (XPS) analysis was performed to analyze the elements in the composition, specifically boron (B), using a Thermo Scientific/K-Alpha Brand XPS Device with monochrome Al K α .

The chemical resistance test of glass fibers was carried out in accordance with the study of Yurdakul et al [10]. To measure the chemical resistance of borosilicate glass fibers in a basic environment, 40 g sodium hydroxide (NaOH) and 1 L of distilled water were mixed. Then, the glass fibers were cut in 5 mm length and added to the solution. Finally, the chemical resistance test was started at 75°C to observe the weight loss.

The thickness measurements of the borosilicate glass fiber were made on the Hitachi SU5000 Scanning Electron Microscopy (SEM) at Yıldırım Beyazıt University, Electron Microscopy Laboratories. During analysis, an acceleration voltage of 10 kV was used at working distances of 8.1 and 9.5 mm.

3. Results and Discussion

3.1. Thermal Analysis

The thermal behavior and mass change of borosilicate glass were investigated by DSC and TG analyses. In the DSC studies to determine the softening point range of borosilicate glasses, it has been observed that the softening point varies between 830-860°C. Due to the fact that the boron content in the glass composition reduces crosslinking, it reduces viscosity. Thus, the glass becomes formable [28,29]. The analysis results are presented in Figure 3. It was observed that 850°C is the softening point of the borosilicate glass. After this temperature, the material became suitable for fiber drawing. With the increase in temperature, weight

loss is observed with the evaporation of the material. The weight loss, which started at 780°C, continued to increase gradually. It was observed that the highest mass loss was experienced, especially around the endothermic peak at 1100°C.

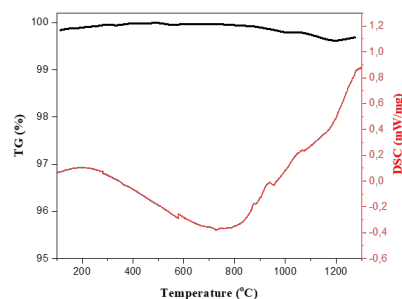


Figure 3. The result of DSC and TG analyses of borosilicate glass.

3.2. Elemental Analysis

XPS analysis was performed to determine the composition of both borosilicate glass fibers obtained after fiber drawing and raw borosilicate glasses. According to the XPS results, the elemental composition of all samples was determined, and they are listed in Table 2.

In the XPS spectra presented in Figure 4, binding energies corresponding Al, Ca, Si, B, O, and Na were observed. The binding energy ranges of B1s, Ca2p, and Na1s are in the range of 182 to 196 eV [30,31], 340 to 360 eV [32,33], and 1062 to 1078 eV [34,35], respectively. There was a reduction in the boron trioxide (B₂O₃), calcium oxide (CaO), and sodium oxide (Na₂O) amounts in the borosilicate glass composition after the fiber drawing process. As shown in Figure 4, significant reduction was observed especially in the relative boron intensities. It was estimated that this reduction is due to relative increase in the evaporation of some of the species in the composition during the

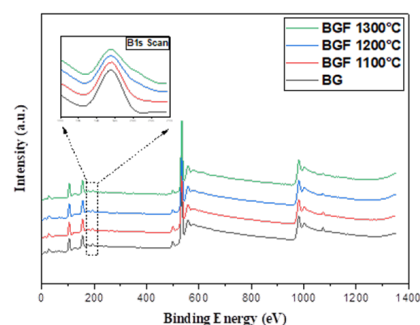


Figure 4. The result of XPS survey analysis of borosilicate glass and fibers produced at different temperatures.

Table 2. The chemical composition (wt%) of borosilicate glass and fibers produced at different temperatures.

Temperature	SiO ₂	Al ₂ O ₃	B ₂ O ₃	CaO	Na ₂ O
Borosilicate Glass (BG)	53.20	9.07	27.75	0.40	9.58
Borosilicate Glass Fiber (BGF) (1100°C)	57.74	12.35	23.67	0.11	6.13
Borosilicate Glass Fiber (BGF) (1200°C)	58.42	12.84	23.06	0.06	5.62
Borosilicate Glass Fiber (BGF) (1300°C)	59.10	13.33	22.45	0.02	5.10

high temperature fiber drawing process. Thus, while the amounts of CaO, Na₂O and B₂O₃ decreased in the final fiber composition, the ratios of silicon dioxide (SiO₂) and aluminum oxide (Al₂O₃) amounts in the composition increased.

The core-level peaks of O1s photoelectron spectrum for borosilicate glass as a result of curve fitting (Figure 5) were analyzed using the CasaXPS software and also Shirley background was used to match peak in the spectrum. The small peak between 534 to 537 eV is a Na Auger peak (Na⁺ ions) [36]. The low and high energy peaks of an O1s signal were attributed to bridging oxide (BO) and non-bridging oxide (NBO) components, respectively [31]. The O1s spectrum was deconvoluted into five individual component peaks centered at 530.9 eV, 531.6 eV, 532.6 eV, 533.1 and 535.1 eV. These correspond to the B-O-Na bond of non-bridging oxide (NBO), and the Si-O-Si and Si-O-Al bonds of bridging oxide (BO) were defined [37,38]. According to the XPS analysis results given in Table 2, it is seen that the amount of B reduces as the temperature increases. The reduction in tetrahedral boron causes an increase in non-bridging oxygens (NBOs) [39]. Therefore, the NBO ratios are lower in borosilicate fibers compared to borosilicate glasses.

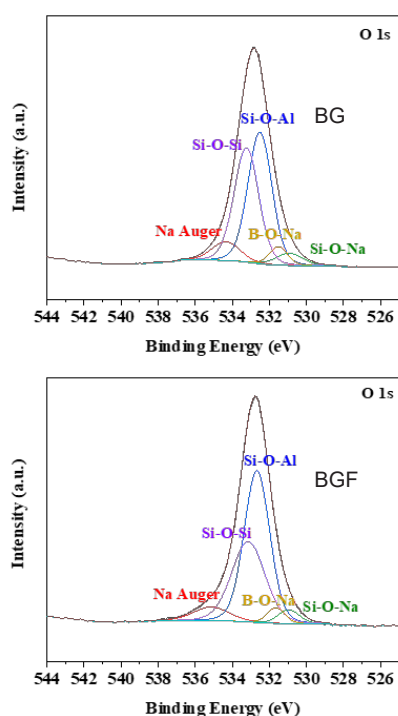


Figure 5. O1s photoelectron spectra and the curve fitting of BG and BGF-1300°C.

3.3. Chemical Resistance Analysis

The weight loss results of borosilicate fibers after 1, 24, 48, and 72 hours from the drawing process can be followed in Figure 6. After 72 hours, 0.53%, 0.48%, and 0.45% mass loss values were calculated at 1100°C, 1200°C and 1300°C, respectively. When the results were examined, it was seen that the weight

loss of borosilicate fibers drawn at 1100°C was higher than the fibers drawn at other temperatures (1200°C and 1300°C). An increase in the surface area was observed due to a decrease in fiber thickness at low temperatures. This increase in the surface area causes a reduction in chemical resistance by increasing the interaction area between NaOH and glass fiber. Fiber thickness decreases with temperature. Thus, it can be concluded that the mass loss will be higher at higher temperature. When the chemical corrosion resistance of glass fibers drawn was compared depending on the surface area, it was seen that glass fibers drawn at 1300°C were very slightly soluble in the NaOH solution (Figure 6).

The chemical resistance of glasses varies depending on the boron and sodium silicate ratios in their composition [40]. The chemical resistance of the fibers is adversely affected by the increase in the ratio of B₂O₃ and Na₂O. According to the XPS analysis results given in Table 2, it is seen that there is a decrease in the amount of both Na and B. Due to the high amount of Na and B in the composition of the glass fibers drawn at 1100°C, more dissolution occurred in the NaOH solution (Figure 6).

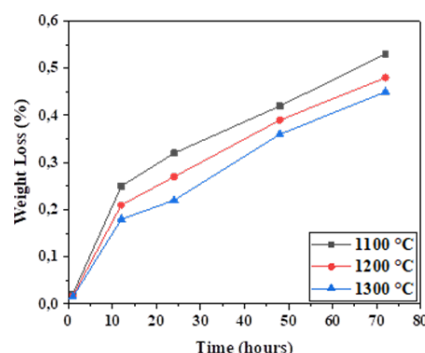


Figure 6. Comparison of chemical resistance test results of fibers drawn at different temperatures.

Another important parameter affecting chemical resistance is the amount of Al₂O₃. Depending on the high alumina ratio in the chemical composition of the glass fibers, some glass properties such as chemical durability can be improved [41,42]. According to the XPS analysis results given in Table 2, while the amount of Al increased with the increasing in fiber drawing temperature, the amounts of B, Ca, and Na decreased.

Therefore, it can be concluded that the chemical resistance is enhanced with the increase in fiber thickness due to the increase in fiber drawing temperature. Also, the chemical durability improved due to reduced amounts of Na and B within the chemical composition of fibers and increasing amount of Al₂O₃.

3.4. The Amount of Feeding Material

In this study, fiber spinning was performed at three different winding speeds (50, 175, 300 rpm) at three distinct temperatures (1100°C, 1200°C, and 1300°C).

Before the fiber drawing started, 115 g of borosilicate glass pieces were added to the crucible. Fiber spinning was done at 1100°C, 1200°C, and 1300°C for 3 hours. Since the viscosity of the material is high at 1100°C, the temperature value is not suitable for fiber drawing. Winding was done at 1100°C with only 50 rpm. After the drawing process was completed, the remaining material amount in the crucible was weighed. The amount of materials that were used during the glass fiber drawing processes are given in Figure 7. It was observed that the amount of material consumed increased with the increase of winding speed and temperature.

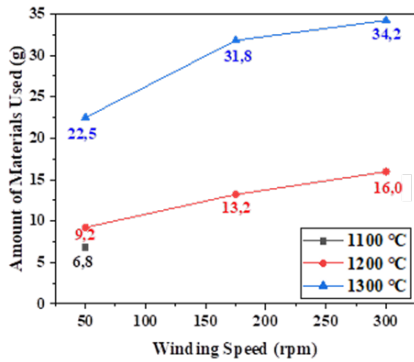


Figure 7. The amount of material used at different temperatures and different winding speeds.

3.5. Measurement of Thickness

The thickness measurements of fibers produced at different temperatures and winding speeds were determined using SEM analyzes. By keeping the amount of material in the crucible constant, the thickness of the fibers was examined at previously mentioned operating temperatures and winding speeds. Measurements of thickness were made at certain time intervals of 10 min, 30 min, 60 min. The images of fibers that are obtained as a result of different parameters are given in Figure 8.

As a result of these measurements, it can be seen that when the amount of feeding material decreased (Figure 7), the fiber thickness decreased from approximately 22 μm to 5-6 μm, as given in Figure 9. It was estimated that these values are observed because the amount of material decrease is too much at 1100°C and 50 rpm rotation speed. Besides, the viscosity of melt which is the other most important parameter on fiber thickness, is increased due to decreasing temperature that is why the material from the nozzles is not enough. This situation results in a significant reduction in fiber thicknesses is observed.

In order to determine the average fiber thickness, 10 measurements were taken per parameter from different fibers. The data of these average values are given in Figure 10.

Fibers were not drawn at 1100°C-300 rpm and 175 rpm winding speeds, which is why the results of these

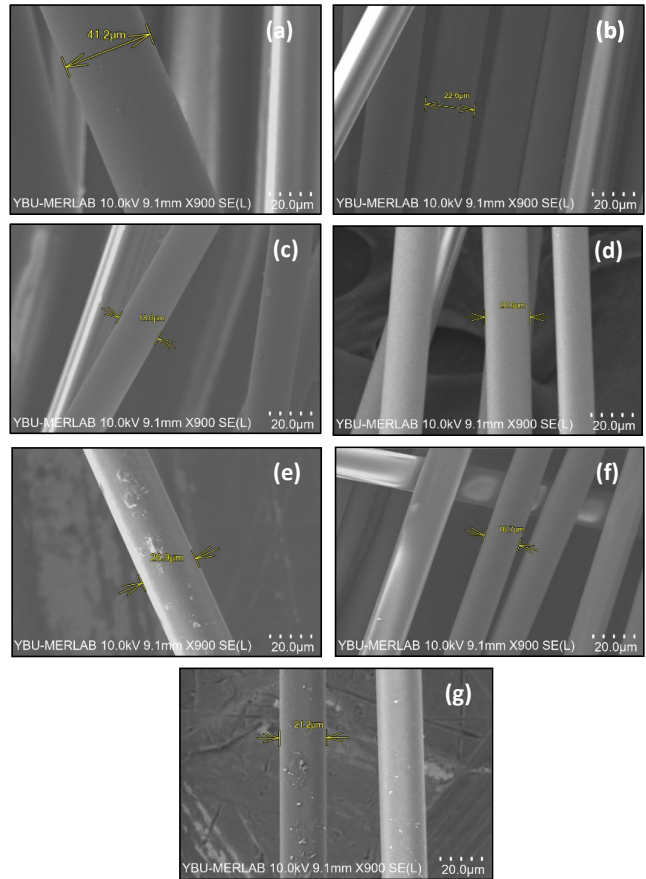


Figure 8. SEM images of fibers at different temperatures and different winding speeds (a) 1300°C-50 rpm-10 min, (b) 1300°C-175 rpm-30 min, (c) 1300°C-300 rpm-1h, (d) 1200°C-50 rpm-10 min, (e) 1200°C-175 rpm-30 min, (f) 1200°C-300 rpm-1h, (g) 1100°C-50 rpm-1h, under 900x magnification (Scale bar: 20 μm).

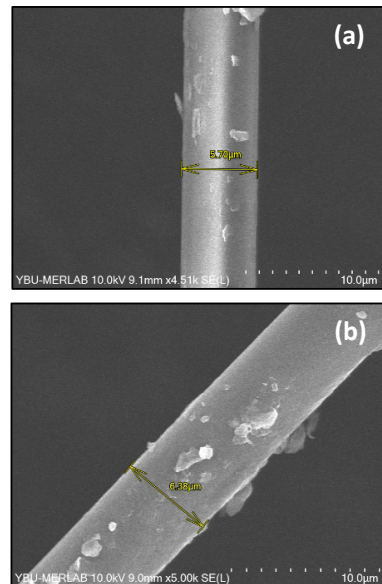


Figure 9. The SEM images of fiber thicknesses at 1100°C-50 rpm-1 hour (a-b) (Scale bar: 10 μm).

parameters are absent in Figure 10a. The viscosity was inadequate at 1100°C. Hence, the rupture was observed in the fibers with the increase of the winding speed, and long-term winding could not be sustained at 1100°C. As can be seen from Figure 10, the thick-

ness of fibers increased as the temperature increased. The reason for this is that the viscosity of the material decreases depending on the temperature. When the winding speed increased at the same temperature value, the fiber thickness decreased due to the decrease in the amount of material.

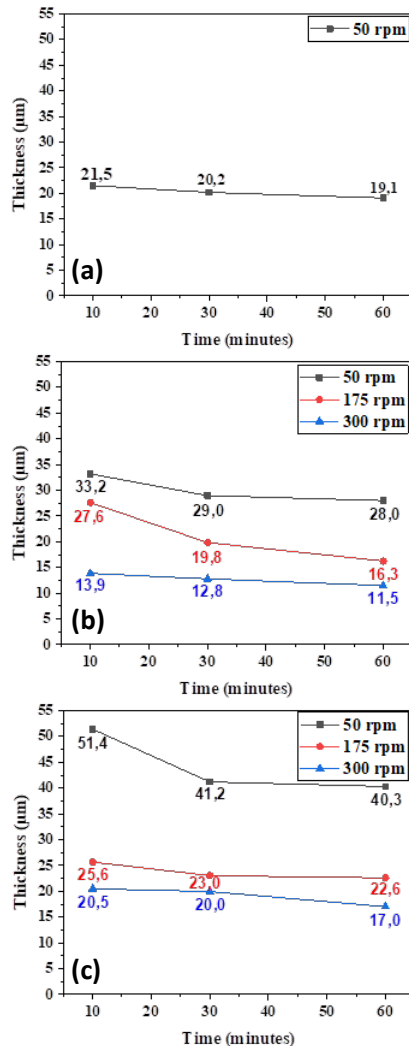


Figure 10. The thickness of borosilicate glass fibers drawn at different temperatures at 1100°C (a), 1200°C (b), and 1300°C (c).

4. Conclusions

The results indicated that 1100°C is not sufficient in terms of viscosity for fiber drawing at 175 rpm and 300 rpm spinning speed, and ruptures occur during fiber drawing. Therefore, studies have been carried out at higher temperatures. As a result of the lower viscosity of the glass composition at 1200°C and 1300°C, fiber drawing was achieved more easily. However, it was observed that evaporation was high at 1300°C, and there was a decrease in the amount of material. From XPS measurements, it is concluded that as the operating temperature increases, the ratios of B_2O_3 , CaO, and Na_2O decreases, except for the SiO_2 and Al_2O_3 . Accordingly, it was observed that the chemical resistance of the glass fibers also changed.

The SEM results clearly presented that fiber thickness decreased as the amount of material in the melting crucible decreased and/or the winding speed increased. It was also observed that as the winding time increased, the amount of material in the crucible decreased, so the fibers were thinner, and even ruptures were detected. According to current findings, it was determined that the best process parameters are 1300°C and 50 rpm.

Acknowledgement

We would like to thank TENMAK-Boron Research Institute and their laboratory staff for their support during this research. We would like to gratefully acknowledge the support of Muhammet Nasuh Arık and Özden Kısacık.

References

- [1] Lowenstein, K. L. (1975). The manufacture of continuous glass fibres present trends in the use of platinum alloys. *Platinum Metals Review*, 19(3), 82-87.
- [2] Cevahir, A. (2017). Fiber Technology for Fiber-Reinforced Composite. *Glass Fibers* (pp. 99-121). Woodhead Publishing. ISBN 978-0-08-101871-2.
- [3] Zou, C., Shi, Y., & Qian, X. (2020). Characterization of glass fiber felt and its performance as an air filtration media. *Journal of Industrial Textiles*, 1528083720961410.
- [4] Jones, F. R., & Huff, N. T. (2018). *The structure and properties of glass fibers*. In *Handbook of Properties of Textile and Technical Fibres* (pp. 757-803). Woodhead Publishing. ISBN: 9780081018866.
- [5] Jones, F. R. (2001). High-Performance Fibres. In Hearle, J. W. (Ed.), *Glass Fibres* (pp. 191-235). Elsevier.
- [6] Bunsell, A. R. (1988). *Fibre Reinforcements for Composite Materials*. North Holland Publishing Co. ISBN 978-0444428011.
- [7] Vallittu, P. K., Närhi, T. O., & Hupa, L. (2015). Fiber glass-bioactive glass composite for bone replacing and bone anchoring implants. *Dental Materials*, 31(4), 371-381.
- [8] Shen, N., Samanta, A., Wang, Q., & Ding, H. (2017). Selective laser melting of fiber-reinforced glass composites. *Manufacturing Letters*, 14, 6-9.
- [9] Liu, S., & Banta, L. E. (2010). Parametric study of glass fiber drawing process. *International Journal of Applied Glass Science*, 1(2), 180-187.
- [10] Yurdakul, A., Gunkaya, G., Dolekcekic, E., Kavas, T., & Karasu, B. (2015). Novel glass compositions for fiber drawing. *Ceramics International*, 41(10), 13105-13114.
- [11] Chouffart, Q. (2018). *Experimental and numerical investigation of the continuous glass fiber drawing process* [Ph.D. Thesis, University of Liège].
- [12] Brøndsted, P., Lilholt, H., & Lystrup, A. (2018). Composite materials for wind power turbine blades. In *Renewable Energy*, 182-216. Routledge.

- [13] Sathishkumar, T. P., Satheeshkumar, S., & Naveen, J. (2014). Glass fiber-reinforced polymer composites-a review. *Journal of Reinforced Plastics and Composites*, 33(13), 1258-1275.
- [14] Ashok Kumar, M., Ramachandra Reddy, G., Siva Bharathi, Y., Venkata Naidu, S., & Naga Prasad Naidu, V. (2010). Frictional coefficient, hardness, impact strength, and chemical resistance of reinforced sisal-glass fiber epoxy hybrid composites. *Journal of Composite Materials*, 44(26), 3195-3202.
- [15] Chandra, D. S., Reddy, K. V. K., & Hebbal, O. (2018). Fabrication and mechanical characterization of glass and carbon fibre reinforced composite's used for marine applications. *International Journal of Engineering & Technology*, 7(4), 228-232.
- [16] Krug Iii, D. J., Asuncion, M. Z., Popova, V., & Laine, R. M. (2013). Transparent fiber glass reinforced composites. *Composites Science and Technology*, 77, 95-100.
- [17] Petersen, H. N., Kusano, Y., Brøndsted, P., & Almdal, K. (2013). Preliminary characterization of glass fiber sizing. *34th Risø International Symposium on Materials Science*. 34, 333-340.
- [18] Nishii, J., Morimoto, S., Inagawa, I., Iizuka, R., Yamashita, T., & Yamagishi, T. (1992). Recent advances and trends in chalcogenide glass fiber technology: a review. *Journal of Non-Crystalline Solids*, 140, 199-208.
- [19] Chouffart, Q., Simon, P., & Terrapon, V. E. (2016). Numerical and experimental study of the glass flow and heat transfer in the continuous glass fiber drawing process. *Journal of Materials Processing Technology*, 231, 75-88.
- [20] Liu, S. (2010). *Process model and control system for the glass fiber drawing process*. West Virginia University.
- [21] Xu, D., Dai, S., You, C., Wang, Y., Han, X., Lin, C., ... & Chen, F. (2017). Optimization of draw processing parameters for As₂Se₃ glass fiber. *Optical Fiber Technology*, 38, 46-50.
- [22] Choudhury, S. R., & Jaluria, Y. (1998). Practical aspects in the drawing of an optical fiber. *Journal of Materials Research*, 13(2), 483-493.
- [23] Cousins, D. S., Suzuki, Y., Murray, R. E., Samaniuk, J. R., & Stebner, A. P. (2019). Recycling glass fiber thermoplastic composites from wind turbine blades. *Journal of Cleaner Production*, 209, 1252-1263.
- [24] Krohn, D. A., & Cooper, A. R. (1969). Strengthening of glass fibers: I, cladding. *Journal of the American Ceramic Society*, 52(12), 661-664.
- [25] Liu, S., & Banta, L. E. (2010). Parametric study of glass fiber drawing process. *International Journal of Applied Glass Science*, 1(2), 180-187.
- [26] Lima, M. M., & Monteiro, R. (2001). Characterisation and thermal behaviour of a borosilicate glass. *Thermochimica Acta*, 373(1), 69-74.
- [27] Gupta, P. K., Lur, M. L., & Bray, P. J. (1985). Boron coordination in rapidly cooled and in annealed aluminum borosilicate glass fibers. *Journal of the American Ceramic Society*, 68(3), C-82.
- [28] Wallenberger, F. T., Watson, J. C., & Li, H. (2000). *Glass Fibers*. PPG Industries. Inc., ASM International, Ohio, USA.
- [29] Karasu, B., Demirel, İ., Aydın, S., Dalkıran, M., & Beyza, L. İ. K. (2020). Past and Present Approaches to Borosilicate Glasses. *El-Cezeri Journal of Science and Engineering*, 7(2), 940-969.
- [30] Kaky, K. M., Şakar, E., Akbaba, U., Kasapoğlu, A. E., Sayyed, M. I., Gür, E., ... & Mahdi, M. A. (2019). X-ray photoelectron spectroscopy (XPS) and gamma-ray shielding investigation of boro-silicate glasses contained alkali/alkaline modifier. *Results in Physics*, 14, 102438.
- [31] Miura, Y., Kusano, H., Nanba, T., & Matsumoto, S. (2001). X-ray photoelectron spectroscopy of sodium borosilicate glasses. *Journal of Non-Crystalline Solids*, 290(1), 1-14.
- [32] Yu, X. G., Gong, Y., Bi, W. Y., Tian, X. C., Ma, H. W., Zhao, H. F., ... & Wang, L. (2008). XPS studies on ZrO₂ thin films deposited on glass substrate by sol-gel. *In Key Engineering Materials*. 368, 1277-1279. Trans Tech Publications Ltd.
- [33] Zhang, Y., Zhang, J., Jin, Y., Zhang, J., Hu, G., Lin, S., ... & Xiang, W. (2017). Construction and nonlinear optical characterization of CuO quantum dots doped Na₂O-CaO-B₂O₃-SiO₂ bulk glass. *Journal of Materials Science: Materials in Electronics*, 28(17), 13201-13208.
- [34] Mekki, A., Holland, D., McConville, C. F., & Salim, M. (1996). An XPS study of iron sodium silicate glass surfaces. *Journal of Non-Crystalline Solids*, 208(3), 267-276.
- [35] Nesbitt, H. W., Bancroft, G. M., & Ho, R. (2017). XPS valence band study of Na-silicate glasses: energetics and reactivity. *Surface and Interface Analysis*, 49(13), 1298-1308.
- [36] Sharma, A., Jain, H., & Miller, A. C. (2001). Surface modification of a silicate glass during XPS experiments. *Surface and Interface Analysis: An International Journal devoted to the development and application of techniques for the analysis of surfaces, interfaces and thin films*, 31(5), 369-374.
- [37] Hsieh, C. H., Jain, H., Miller, A. C., & Kamitsos, E. I. (1994). X-ray photoelectron spectroscopy of Al- and B-substituted sodium trisilicate glasses. *Journal of Non-Crystalline Solids*, 168(3), 247-257.
- [38] Hubert, M., & Faber, A. J. (2014). On the structural role of boron in borosilicate glasses. *Physics and Chemistry of Glasses-European Journal of Glass Science and Technology Part B*, 55(3), 136-158.
- [39] Angeli, F., Villain, O., Schuller, S., Charpentier, T., de Ligny, D., Bressel, L., & Wondraczek, L. (2012). Effect of temperature and thermal history on borosilicate glass structure. *Physical Review B*, 85(5), 054110.
- [40] Jones, F. R., & Huff, N. T. (2018). The structure and

properties of glass fibers. In *Handbook of Properties of Textile and Technical Fibres*. 757-803. Woodhead Publishing.

- [41] Tait, J. C., & Mandolesi, D. L. (1983). *The chemical durability of alkali aluminosilicate glasses* (No. AECL-7803). Atomic Energy of Canada Ltd.
- [42] Liu, H., Yang, R., Wang, Y., & Liu, S. (2013). Influence of alumina additions on the physical and chemical properties of lithium-iron-phosphate glasses. *Physics Procedia*, 48, 17-22.